Chinese Journal of
POLYMER SCIENCE

ARTICLE

https://doi.org/10.1007/s10118-021-2622-z
Chinese J. Polym. Sci. **2021**, *39*, 1489–1495

A Unified Thermodynamic Model of Flow-induced Crystallization of Polymer

Cui Nie, Fan Peng, Ting-Yu Xu, Jun-Fang Sheng*, Wei Chen, and Liang-Bin Li*

National Synchrotron Radiation Laboratory, Anhui Provincial Engineering Laboratory of Advanced Functional Polymer Film, CAS Key Laboratory of Soft Matter Chemistry, University of Science and Technology of China, Hefei 230026, China

Abstract We propose a unified thermodynamic model of flow-induced crystallization of polymer (uFIC), which incorporates not only the conformational entropy reduction but also the contributions of flow-induced chain orientation, the interaction of ordered segments, and the free energy of crystal nucleus and crystal morphology. Specifically, it clarifies the determining parameters of the critical crystal nucleus size, and is able to account for the acceleration of nucleation, the emergence of precursor, different crystal morphologies and structures induced by flow. Based on the nucleation barrier under flow, we analyze at which condition precursor may occur and how flow affects the competition among different crystal forms such as orthorhombic and hexagonal phases of polyethylene. According to the uFIC model, the different crystal morphologies and structures in the flow-temperature space have been clarified, which give a good agreement with experiments of FIC.

Keywords Flow-induced crystallization; Unified thermodynamic model; Flow-induced chain orientation

Citation: Nie, C.; Peng, F.; Xu, T. Y.; Sheng, J. F.; Chen, W.; Li, L. B. A unified thermodynamic model of flow-induced crystallization of polymer. *Chinese J. Polym. Sci.* **2021**, *39*, 1489–1495.

INTRODUCTION

Flow- or strain-induced crystallization (FIC or SIC) of polymers occurs not only in processing like film blowing, injection molding and fiber spinning, but also in service of some polymers like natural rubber and shape memory materials.[1−5] Though large efforts from both academic and industrial communities have been devoted for understanding FIC, it still remains as a classic and important challenge in polymer physics.[5,6] In recent two decades, new techniques such as *in situ* synchrotron radiation X-ray scattering and computer simulations provide more in-depth information about the kinetic pathway of FIC, but we still lack a thermodynamic theory of FIC to incorporate these new observations, such as the mesophase or precursor, shish-kebab, and the emergence of new crystal forms.[7−15]

At present, Flory's conformational entropy reduction model (CERM) proposed in 1947 is the most widely recognized model for FIC, which was originated from uniaxial stretching of natural rubber.[16] CERM depicts a process of flow-induced chain straightening, which results in conformational entropy reduction (CER, ΔS_{con}) of melt. Based on the classic nucleation theory (see Fig. 1a), CERM simply incorporates ΔS_{con} (see Fig. 1b) and expresses the nucleation barrier under flow $\Delta G_{\mathrm{f}}^{*}$ as

$$\Delta G_{\mathrm{f}}^{*} = \Delta G_{0}^{*} + T\Delta S_{\mathrm{con}} \tag{1}$$

where ΔG_{0}^{*} represents the nucleation barrier at quiescent condition. As ΔS_{con} is negative, thus $\Delta G_{\mathrm{f}}^{*} < \Delta G_{0}^{*}$, namely the

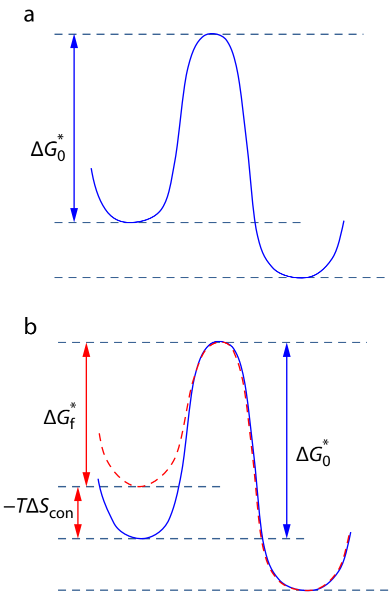

Fig. 1 Schematic illustration of the free energy barrier of nucleation (a) at quiescent condition and (b) under flow from the conformational entropy reduction (CERM) model. ΔG_{0}^{*} and $\Delta G_{\mathrm{f}}^{*}$ are the nucleation barrier at quiescent condition and under flow; ΔS_{con} is the conformational entropy reduction of melt induced by flow.

---

* Corresponding authors, E-mail: jfsheng@ustc.edu.cn (J.F.S.)
E-mail: lbli@ustc.edu.cn (L.B.L.)

Received May 7, 2021; Accepted June 21, 2021; Published online August 3, 2021

nucleation barrier is reduced. Correspondingly, the equilibrium melting temperature T^0_{mf} of the crystal increases under flow, which can be written as

$$\frac{1}{T^0_{\mathrm{mf}}}=\frac{1}{T^0_{\mathrm{m}}}-\frac{\Delta S_{\mathrm{con}}}{\Delta H} \tag{2}$$

where T^0_{m} and ΔH are the equilibrium melting temperature and the crystallization enthalpy of the crystal at quiescent condition, respectively. CERM can qualitatively account for flow-induced enhancement of nucleation rate and has been widely employed to explain FIC experiments and simulations.[12−14] Later on, although various expressions of ΔS_{con} have been introduced by different groups and chain dynamics of polymer without crosslink is also considered, new models keep the essential physics of CERM and take ΔS_{con} as the core contributor in understanding FIC.[17−19]

Conformational entropy is a global parameter on the individual chains, while nucleation and crystallization are packing processes involving local multi-chain segments, suggesting that ΔS_{con} may not be the most important contributor in FIC. Indeed, CERM misses several important physics observed in experiments and simulations.[20−25] Fig. 2 presents a schematic illustration of the factors modified by flow. Starting from the classic nucleation theory with liquid and crystal states, we first examine what happen in the initial polymer liquid under flow. (i) Chain orientation. Chain straightening or ΔS_{con} only considers individual chains and does not take chain orientation or parallel packing involving multi-chain segments into account, while parallel packing of segments is inevitably required in crystal nucleation. In uniaxial flow, the chain straightening and chain orientation occur synchronously, leading to little attention on the effect of orientation on FIC for a long period. However, a recent discovery about the frustrating SIC of natural rubber during biaxial stretching has suggested the crucial role of chain orientation on FIC.[20] Therefore, in addition to ΔS_{con}, entropy change related to orientation ΔS_{ori} should be put into the theory of FIC separately. (ii) Chain interaction. Flow-induced preordering or precursor has been widely reported in FIC experiments, in which non-crystalline shish detected with *in situ* X-ray scattering is a representative example.[9,26] These experimental observations reveal that not only entropy but also enthalpy or molecular interactions are changed by flow. Thus flow-induced enthalpy change of polymer liquid $\Delta H^{\mathrm{l}}_{\mathrm{f}}$ should be considered in FIC theory. After depicting the initial liquid, we then shift our attention to the final crystalline state. (iii) Crystal morphology and structure. Flow modifies crystal morphology (*e.g.*, from lamellae to shish-kebab) and crystal form (*e.g.*, from orthorhombic to hexagonal crystals for polyethylene (PE)) has been largely documented since the earliest FIC study,[27−33] but historically, these factors had been surprisingly overlooked in FIC theory. If flow induces new crystal forms, enthalpy difference $\Delta H^{\mathrm{c}}_{\mathrm{f}}$ between crystals at quiescent and strained conditions should be introduced. Meanwhile, transforming crystal morphology from lamellae to shish should change the free energy density of end surface, that is, from folded-chain surface σ_{e} to extended-chain surface σ_{ef}. Evidently, in addition to ΔS_{con} in CERM, the new FIC theory should consider the above three factors.

Based on the experiment and simulation results, FIC models incorporating the effects of orientation, chain interaction, new crystal morphology and structure have been proposed in recent years, which, however, were considered separately. Chen *et al.*[20] introduced the orientation entropy and the

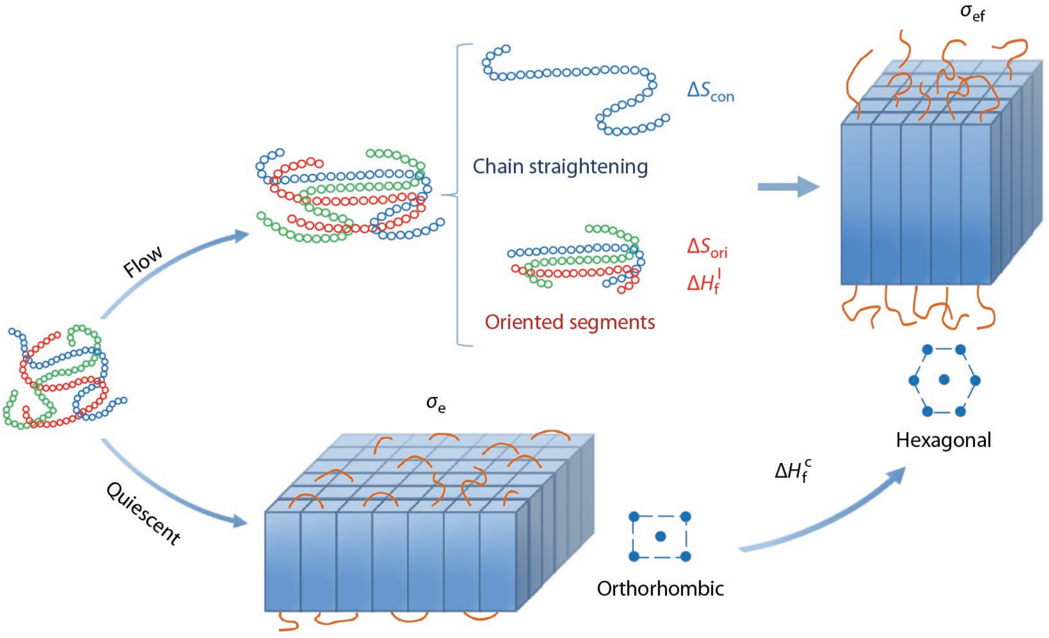

Fig. 2 Flow-induced changes of the physical parameters in FIC. ΔS_{con} and ΔS_{ori} are the entropy change of conformation and orientation of melt induced by flow; $\Delta H^{\mathrm{l}}_{\mathrm{f}}$ is the enthalpy change of polymer melt due to the interaction of ordered segments; $\Delta H^{\mathrm{c}}_{\mathrm{f}}$ is the enthalpy difference between two crystal forms like flow-induced orthorhombic and hexagonal phases of PE; σ_{e} and σ_{ef} are the free energy densities of crystal end surface at quiescent condition and under flow.

chain interaction between the ordered segments, while Liu *et al.*[24] took the free energy change of the final crystalline state into account and proposed the entropy reduction-energy change (ER-EC) model. Although these efforts make a stepwise progress for understanding FIC, a unified FIC theory incorporating the above three factors has not been developed yet.

In this work, starting from classic nucleation theory, we propose a thermodynamic model for FIC to unify flow-induced changes of conformational entropy $\Delta S_{\rm con}$, orientation entropy $\Delta S_{\rm ori}$, chain interaction of polymer liquid $\Delta H_{\rm f}^{\rm l}$, and modifications of crystal structure $\Delta H_{\rm f}^{\rm c}$ and morphology $\sigma_{\rm ef}$. Our model is a thermodynamically phenomenological model but explicitly unifies all structural changes in FIC study. For the convenience of description, we name it as uFIC model hereafter. The possible calculation methods for the changes of conformational entropy $\Delta S_{\rm con}$, orientation entropy $\Delta S_{\rm ori}$ and chain interaction of polymer liquid $\Delta H_{\rm f}^{\rm l}$ are given in the Appendix, as they have been discussed in early studies.[16,20]

THEORY AND METHOD

To deduce the uFIC model, we first incorporate flow-induced variations of entropy and enthalpy into the chemical potential $\mu = H - TS$. The chemical potential difference per unit volume between polymer crystal and melt (liquid) phases under flow can be written as

$$\Delta\mu_{\rm f} = \Delta H_{\rm f} - T\Delta S_{\rm f} = \Delta H + \Delta H_{\rm f}^{\rm c} - \Delta H_{\rm f}^{\rm l} - T(\Delta S - (\Delta S_{\rm con} + \Delta S_{\rm ori})) \quad (3)$$

where ΔH and $\Delta H_{\rm f} = \Delta H + \Delta H_{\rm f}^{\rm c} - \Delta H_{\rm f}^{\rm l}$ are the crystallization enthalpies of polymer melt at quiescent condition and under flow, respectively. While ΔS and $\Delta S_{\rm f} = \Delta S - (\Delta S_{\rm con} + \Delta S_{\rm ori})$ are the crystallization entropies of polymer melt at quiescent condition and under flow, respectively. Here, the contribution of conformation and orientation to the entropy change of the melt are considered. Note in current work, the symbols with subscript "f" represent the physical parameters under flow. In Eq. (3), we assume that the difference in the entropies of crystal phase between quiescent and strained conditions is negligible. At the equilibrium melting temperature under flow $T_{\rm mf}^0$, the chemical potential of these two phases is equal, $\Delta\mu_{\rm f} = 0$, which results in

$$T_{\rm mf}^0 = \frac{\Delta H_{\rm f}}{\Delta S_{\rm f}} = \frac{\Delta H + \Delta H_{\rm f}^{\rm c} - \Delta H_{\rm f}^{\rm l}}{\Delta S - (\Delta S_{\rm con} + \Delta S_{\rm ori})} \quad (4)$$

Then, Eq. (3) can be written as

$$\Delta\mu_{\rm f} = \Delta H_{\rm f}\left(1 - \frac{T}{T_{\rm mf}^0}\right) = \frac{\Delta H_{\rm f}\Delta T_{\rm f}}{T_{\rm mf}^0} \quad (5)$$

where $\Delta T_{\rm f}$ is the supercooling under flow. Inserting $T_{\rm m}^0 = \dfrac{\Delta H}{\Delta S}$ into Eq. (4) and taking the reciprocal lead to the following equation

$$\frac{1}{T_{\rm mf}^0} = \frac{\Delta H}{\Delta H_{\rm f} T_{\rm m}^0} - \frac{\Delta S_{\rm con} + \Delta S_{\rm ori}}{\Delta H_{\rm f}} \quad (6)$$

The CERM and other FIC models generally assume that the free energies of the critical nucleus and the final state under flow keep the same as those at quiescent condition. However, at the same crystallization temperature $T_{\rm c}$, the size of the critical crystal nucleus should decrease as the equivalent supercooling under flow is expected to increase. Obviously, the free energy landscape changes under flow, which will be considered in our uFIC model (see Fig. 3a). Following the classical nucleation theory,[34] the free energy change for the formation of a cylindrical crystal nucleus from the liquid phase under flow is given by

$$\Delta G_{\rm f} = \pi R^2 L\Delta\mu_{\rm f} + 2\pi RL\sigma_{\rm sf} + 2\pi R^2\sigma_{\rm ef} \quad (7)$$

where $\sigma_{\rm ef}$ and $\sigma_{\rm sf}$ are the free energy densities for the end and side surfaces of a cylindrical nucleus of length L and radius R under flow, $\Delta\mu_{\rm f}$ is the chemical potential difference per unit volume between the crystal and melt phases under flow. Combining Eq. (5), the critical nucleus thickness $L_{\rm cf}$ and the critical nucleus radius $R_{\rm cf}$ are obtained by finding the maximum in $\Delta G_{\rm f}$ with respect to nucleus length L and nucleus radius R in Eq. (7),

$$\begin{cases} L_{\rm cf} = -\dfrac{4\sigma_{\rm ef}T_{\rm mf}^0}{\Delta H_{\rm f}\Delta T_{\rm f}} = K_{\rm L}L_{\rm c} = -K_{\rm L}\dfrac{4\sigma_{\rm e}T_{\rm m}^0}{\Delta H\Delta T} \\ R_{\rm cf} = -\dfrac{2\sigma_{\rm sf}T_{\rm mf}^0}{\Delta H_{\rm f}\Delta T_{\rm f}} = K_{\rm R}R_{\rm c} = -K_{\rm R}\dfrac{2\sigma_{\rm s}T_{\rm m}^0}{\Delta H\Delta T} \end{cases} \quad (8)$$

where we assume that the ratios of these two values to the length $L_{\rm c}$ and radius $R_{\rm c}$ of the critical nucleus at quiescent condition are $K_{\rm L}$ and $K_{\rm R}$, respectively. Then the free energy densities of the end and side surfaces of crystals under flow can be obtained as

$$\begin{cases} \sigma_{\rm ef} = K_{\rm L}\dfrac{T_{\rm m}^0}{T_{\rm mf}^0}\dfrac{\Delta H_{\rm f}\Delta T_{\rm f}}{\Delta H\Delta T}\sigma_{\rm e} \\ \sigma_{\rm sf} = K_{\rm R}\dfrac{T_{\rm m}^0}{T_{\rm mf}^0}\dfrac{\Delta H_{\rm f}\Delta T_{\rm f}}{\Delta H\Delta T}\sigma_{\rm s} \end{cases} \quad (9)$$

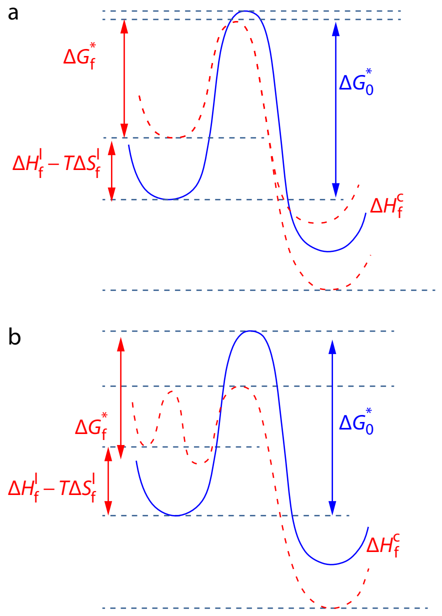

Fig. 3 Schematic illustration of the free energy barrier of nucleation under flow. (a) The uFIC model incorporates the entropy change of polymer melt originated from conformation and orientation $\Delta S_{\rm f}^{\rm l} = \Delta S_{\rm con} + \Delta S_{\rm ori}$, enthalpy change of polymer melt $\Delta H_{\rm f}^{\rm l}$ due to oriented segments and the free energy change of final nucleus with different crystal morphologies and structures induced by flow $\Delta H_{\rm f}^{\rm c}$. (b) The condition for the existence of a thermodynamically metastable intermediate phase under flow.

Substituting these expressions of L_{cf} and R_{cf} into Eq. (7) leads to the free energy barrier of critical crystal nucleus under flow as

$$\Delta G_f^* = \frac{8\pi\sigma_{ef}(\sigma_{sf})^2(T_{mf}^0)^2}{(\Delta H_f)^2(\Delta T_f)^2} \tag{10}$$

Inserting σ_{ef} and σ_{sf} of Eq. (9) into Eq. (10), we have the nucleation barrier of critical nucleus under flow as

$$\Delta G_f^* = K\left(1 + \frac{1}{\Delta\mu_0}\left(\Delta H_f^c - \Delta H_f^l\right) + \frac{1}{\Delta\mu_0}T(\Delta S_{con} + \Delta S_{ori})\right)\Delta G_0^* \tag{11}$$

where ΔG_0^* and $\Delta\mu_0$ are the nucleation barrier of critical nucleus and the chemical potential difference per unit volume between polymer crystal and melt (liquid) phases at quiescent condition, respectively. We also inform a shape factor K as

$$K = K_L K_R^2 = \frac{V_{cf}}{V_c} \tag{12}$$

where V_c and V_{cf} are the volume of critical cylindrical nucleus at quiescent condition and under flow, respectively. According to Eq. (3) and Eq. (9), Eq. (11) can be further written as

$$\Delta G_f^* = \left(\frac{\sigma_{ef}}{\sigma_e}\right)\left(\frac{\sigma_{sf}}{\sigma_s}\right)^2\left(\frac{\Delta\mu_0}{\Delta\mu_f}\right)^2\Delta G_0^* \tag{13}$$

DISCUSSION

As the uFIC model takes both flow-induced modifications of liquid and crystal into account, it is expected that this model can explain all the experimental observations of FIC. To analyze how flow affects nucleation process, we compare the nucleation barriers at flow and quiescent conditions. Here we assume the free energy density of the crystal side surface under flow is unchanged, $\frac{\sigma_{sf}}{\sigma_s} = 1$, then the ratio of the nucleation barriers between these two conditions is

$$\frac{\Delta G_f^*}{\Delta G_0^*} = \left(\frac{\sigma_{ef}}{\sigma_e}\right)\left(\frac{\Delta\mu_0}{\Delta\mu_f}\right)^2 \tag{14}$$

Taking the nucleation barrier expressed in Eq. (14) as the basic starting point, we are going to discuss the 4 characteristic observations in FIC experiments: (i) accelerating nucleation; (ii) changing the nucleus from lamellae to shish; (iii) preordering; and (iv) inducing new crystal form.

(i) Accelerating Nucleation

If we assume flow only changes the melt entropy, Eq. (14) can be re-written as

$$\frac{\Delta G_f^*}{\Delta G_0^*} = \left(\frac{\sigma_{ef}}{\sigma_e}\right)\left[1 - \frac{T(\Delta S_{con} + \Delta S_{ori})}{\Delta\mu_0 + T(\Delta S_{con} + \Delta S_{ori})}\right]^2 \tag{15}$$

Below the equilibrium melting temperature ($\Delta T > 0$), $\Delta\mu_0 < 0$. The molecular chain is stretched and oriented by flow, $(\Delta S_{con} + \Delta S_{ori}) < 0$, $1 - \frac{T(\Delta S_{con} + \Delta S_{ori})}{\Delta\mu_0 + T(\Delta S_{con} + \Delta S_{ori})} < 1$. Under a relative weak flow, free energy density of the end surface of crystal keeps the same as that at quiescent condition, namely $\frac{\sigma_{ef}}{\sigma_e} = 1$, then $\frac{\Delta G_f^*}{\Delta G_0^*} < 1$. Here we should notice that besides decreasing the nucleation barrier, flow can also enhance the movement ability of polymer segments along the stretching direction, which would lead to the increase of the pre-factor of the nucleation rate. Both the two could lead to a higher nucleation rate as observed in FIC experiments and simulations.[10−13,35−37] As the flow strength increases, the degree of molecular chain stretching increases, which can transform the crystal nucleus from lamellae to fringed micellar structure.[38] Owning to the end surface crowding effect of the fringed micellar structure, it has a larger surface free energy, $\frac{\sigma_{ef}}{\sigma_e} > 1$, which would have some hindering effects on FIC. When the external flow is sufficient strong that the crowding effect on the crystal surface has the opportunity to be counteracted by the tensile stress on the molecular chain, the free energy density of end surface is reduced. Here, the crystal morphology and structure may change, which will be discussed below. At $\Delta T < 0$ ($\Delta\mu_0 > 0$), namely FIC occurs at $T_c > T_m^0$ (but $T_c < T_{mf}^0$), $\frac{\Delta G_f^*}{\Delta G_0^*} < 1$ requires $T(\Delta S_{con} + \Delta S_{ori}) < -\Delta\mu_0$, which supports that the deformation exceeding the critical strain is a necessary condition for FIC to occur at $\Delta T < 0$.

(ii) Changing the Nucleus from Lamellae to Shish

Considering that the free energy density of the crystal end surface increases due to the external flow, $\frac{\sigma_{ef}}{\sigma_e} > 1$, but the crystal form does not change, then the transformation from lamellar to shish nucleus can occur. The dimension of a nucleus in different directions is proportional to the free energy density of its perpendicular surface[34] and $\frac{\sigma_{sf}}{\sigma_s} \approx 1$, then according to Eq. (9), the shape factor K can be written as

$$K = \left(\frac{\sigma_{ef}}{\sigma_e}\right)\left(\frac{\Delta\mu_0}{\Delta\mu_f}\right)^3 = \left(\frac{L_f}{L_0}\right)\left(\frac{\Delta\mu_0}{\Delta\mu_f}\right)^3 = \frac{L_f R_f{}^2}{L_0 R_0{}^2} \tag{16}$$

Here, combined with Eq. (3), we clarify the determinants of the critical crystal nucleus size, including conformational entropy change ΔS_{con}, orientation entropy change ΔS_{ori}, enthalpy change of polymer melt ΔH_f^l and crystal ΔH_f^c, and crystal morphology σ_{ef}. And compared with Eq. (14), under flow, $\frac{\Delta\mu_0}{\Delta\mu_f} < 1$, then $K < \frac{\Delta G_f^*}{\Delta G_0^*}$, which means that the critical crystal nucleus size is more reduced than the nucleation barrier under flow, and this is consistent with the results of simulation.[10]

Taking a lamellar nucleus with L_0 = 20 nm and R_0 = 10 nm at quiescent condition, if $\Delta\mu_f$ in FIC is twice as much as $\Delta\mu_0$ at quiescent condition, R_f will be 3.5 nm. Here, owning to the surface crowding effect, we assume that $\frac{\sigma_{ef}}{\sigma_e} = 5$, then $K = \frac{5}{8}$ and the L_{cf} increases to 100 nm in the scale of shish observed in FIC. This simple estimation is reasonable as compared with experimental observations.[24] Obviously, to meet the precondition of $\frac{\sigma_{ef}}{\sigma_e} = 5$, the applied flow field must reach a certain strength, that is, only when the strain or strain rate is sufficiently high can shish-like crystalline structure be formed.

(iii) Preordering

If a precursor emerges in FIC with no change of the final crystal form, which may be either a transient kinetic state or a thermodynamic metastable phase corresponding to a free energy local minimum, the ratio of nucleation barriers is

$$\frac{\Delta G_{\mathrm{f}}^{*}}{\Delta G_{0}^{*}}=\left(\frac{\sigma_{\mathrm{ef}}}{\sigma_{\mathrm{e}}}\right)\left[1+\frac{\Delta H_{\mathrm{f}}^{\mathrm{l}}-T(\Delta S_{\mathrm{con}}+\Delta S_{\mathrm{ori}})}{\Delta\mu_{0}-\left(\Delta H_{\mathrm{f}}^{\mathrm{l}}-T(\Delta S_{\mathrm{con}}+\Delta S_{\mathrm{ori}})\right)}\right]^{2} \tag{17}$$

Obviously, when FIC occurs, $\Delta\mu_{0}-\left(\Delta H_{\mathrm{f}}^{\mathrm{l}}-T(\Delta S_{\mathrm{con}}+\Delta S_{\mathrm{ori}})\right)=\Delta\mu_{\mathrm{f}}<0$. Here, the change of the free energy density of the crystal end surface under flow needs to be considered separately. (i) $\frac{\sigma_{\mathrm{ef}}}{\sigma_{\mathrm{e}}}<1$. The chains in pre-ordered structure are arranged in parallel and retain some freedom of its own axes. Compared with the crystal-melt interface, the density and enthalpy difference between pre-ordered structure and the melt is smaller, which results in a smaller free energy density.[39] Therefore, the condition of $\Delta H_{\mathrm{f}}^{\mathrm{l}}-T(\Delta S_{\mathrm{con}}+\Delta S_{\mathrm{ori}})<0$ may occur (see Fig. 3b), which supports that the precursor is a thermodynamically metastable phase. The occurence of this metastable precursor has been observed in FIC experiments on polyethylene and other polymers,[7,40] which can be qualitatively understood with current uFIC model as discussed above. ii) $\frac{\sigma_{\mathrm{ef}}}{\sigma_{\mathrm{e}}}>1$. The fringed micellar structure of crystal nucleus is induced by strong flow, with an extended-chain surface of higher free energy density. So the condition for acceleration of nucleation $\left(\frac{\Delta G_{\mathrm{f}}^{*}}{\Delta G_{0}^{*}}<1\right)$ requires $\Delta H_{\mathrm{f}}^{\mathrm{l}}-T(\Delta S_{\mathrm{con}}+\Delta S_{\mathrm{ori}})>0$. Here, the precursor is thermodynamically unfavorable as compared with polymer melt, which however may still occur as a transient kinetic state under flow.

(iv) Inducing New Crystal Form

Finally we consider the situation with the competition between two crystal forms like flow-induced orthorhombic and hexagonal phases of PE, where $\Delta H_{\mathrm{f}}^{\mathrm{c}}>0$. According to Eq. (13), the ratio between their nucleation barriers is written as

$$\frac{\Delta G_{\mathrm{hf}}^{*}}{\Delta G_{\mathrm{of}}^{*}}=\left(\frac{\sigma_{\mathrm{ef}}^{\mathrm{h}}}{\sigma_{\mathrm{ef}}^{\mathrm{o}}}\right)\left(\frac{\Delta\mu_{\mathrm{of}}}{\Delta\mu_{\mathrm{hf}}}\right)^{2}=\left(\frac{\sigma_{\mathrm{ef}}^{\mathrm{h}}}{\sigma_{\mathrm{ef}}^{\mathrm{o}}}\right)\left(1-\frac{\Delta H_{\mathrm{f}}^{\mathrm{c}}}{\Delta\mu_{\mathrm{hf}}}\right)^{2} \tag{18}$$

where $\Delta G_{\mathrm{of}}^{*}$ ($\Delta G_{\mathrm{hf}}^{*}$) is nucleation barrier of orthorhombic (hexagonal) phase under flow, $\Delta\mu_{\mathrm{of}}$ ($\Delta\mu_{\mathrm{hf}}$) is the chemical potential difference per unit volume between orthorhombic (hexagonal) crystal and polymer melt under flow, and $\sigma_{\mathrm{ef}}^{\mathrm{o}}$ $\left(\sigma_{\mathrm{ef}}^{\mathrm{h}}\right)$ is the free energy density of orthorhombic (hexagonal) crystal end surface under flow. Obviously, $\Delta\mu_{\mathrm{hf}}<0$ in FIC, as $\Delta H_{\mathrm{f}}^{\mathrm{c}}>0$, and then $1-\frac{\Delta H_{\mathrm{f}}^{\mathrm{c}}}{\Delta\mu_{\mathrm{hf}}}>1$. According to the relationship of ratio $\frac{\sigma_{\mathrm{e}}}{\Delta H}$ and the crystallization enthalpy ratio between orthorhombic phase and hexagonal phase, $\left(\frac{\sigma_{\mathrm{e}}}{\Delta H}\right)_{\mathrm{o}}=3.5\left(\frac{\sigma_{\mathrm{e}}}{\Delta H}\right)_{\mathrm{h}}$ and $\frac{\Delta H_{\mathrm{h}}}{\Delta H_{\mathrm{o}}}=\frac{1}{3}$,[41–43] then $\frac{\sigma_{\mathrm{ef}}^{\mathrm{h}}}{\sigma_{\mathrm{ef}}^{\mathrm{o}}}=\frac{1}{10.5}$. Therefore, the condition for favorable formation of the hexagonal phase $\left(\frac{\Delta G_{\mathrm{hf}}^{*}}{\Delta G_{\mathrm{of}}^{*}}<1\right)$ requires $\Delta\mu_{\mathrm{hf}}<-0.45\Delta H_{\mathrm{f}}^{\mathrm{c}}$. Combining Eq. (16), the relationship between $\Delta\mu_{\mathrm{f}}$ and the critical nucleus size, it proves that for a significantly smaller critical nucleus size, the hexagonal phase is a thermodynamically stable phase, which is in good agreement with early reports.[41] In addition, the driving force $|\Delta\mu_{\mathrm{hf}}|$ required for nucleation increases with temperature, indicating that there is a critical temperature T_{h}, above which the hexagonal phase is more stable than the orthorhombic phase. Based on the above discussion, the crystal morphologies and structures in the flow-temperature space can be constructed, as shown in Fig. 4. As the temperature increases, the required deformation is increased for FIC to occur. And, taking PE as an example, the crystal morphology and structure gradually changes from orthorhombic lamellar crystal to orthorhombic shish crystal, and finally to hexagonal shish crystal at $T>T_{\mathrm{h}}$. This result agrees reasonably well with FIC experiments of PE.[24]

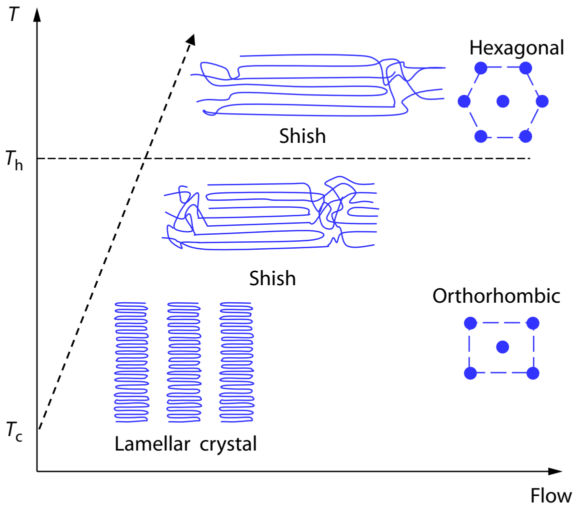

Fig. 4 Schematic illustration of the crystal morphologies and structures of PE in the flow-temperature space.

The above discussion is qualitative and based on some reasonable assumptions, which, however, demonstrates the capability of the uFIC model on understanding experimental observations. The CERM may be numerically applied to fit the flow accelerated nucleation rate, but experimental result suggests ΔS_{con} may make a weak contribution on this effect.[20] Moreover, other observations of FIC, such as precursor, new crystal forms and morphologies have never been considered in the CERM. Through introducing the changes of orientation entropy ΔS_{ori}, chain interaction of polymer liquid $\Delta H_{\mathrm{f}}^{\mathrm{l}}$, the modifications of crystal structure $\Delta H_{\mathrm{f}}^{\mathrm{c}}$ and morphology σ_{ef}, uFIC can not only specify the physical origins for accelerating nucleation rate, but also account for almost all experimental observations in FIC. The above discussion only refers to some specific cases, and the uFIC can be employed to explain other observations of FIC experiments and simulations.

CONCLUSIONS

Taking all the changes of chain conformation, chain orientation, interaction of ordered segments in the initial polymer melt, and the final crystal morphology and structure into account, we propose a uFIC model and rewrite the expression of nucleation free energy barrier under flow, as presented in Eq. (13). Our model can not only effectively explain the flow-accelerated polymer nucleation, but also offer understandings of other FIC experimental observations. It theoretically verifies that the intermediate phase or precursor is a metastable phase only when the free energy density of the interface between the preordering and the melt is smaller than that of the crystal-melt interface. Based on the nucleation barrier under flow, the competition of different crystal forms in the flow can be clarified. Taking PE as an example, the critical transition temperature between orthorhombic and hexagonal crystal forms can be determined by comparing the crystallization enthalpy and the end surface free energy density. In conclusion, our model has the potential to be applied to explain all the observations of FIC experiments which have been done before and can provide a theoretical guidance for further FIC study.

APPENDIX

The estimation of ΔS_{con} has been proposed by different authors with different models.[44−46] Here we take the simple one proposed by Flory.[16] At quiescent condition, the relative coordination of chain ends of the equilibrium polymer melt is approximately considered to obey the Gaussian distribution. Under flow, the amorphous molecular chains are straightened and deviate from the random configurations, resulting in the decrease of conformational entropy. Based on Flory's CERM model, the conformational entropy reduction ΔS_{con} can be expressed as

$$\Delta S_{\text{con}} = 8N_{\text{c}}k_{\text{B}}\left(\beta/\pi^{1/2}\right)^3 \iiint \exp\left[-\beta^2\left(\frac{x^2}{\lambda_x^2}+\frac{y^2}{\lambda_y^2}+\frac{z^2}{\lambda_z^2}\right)\right]\times \left\{A' - \beta^2\left(\frac{n}{n-\xi}\right)\left[x'^2+y'^2+z'^2\right]\mathrm{d}x\mathrm{d}y\mathrm{d}z - N_{\text{c}}k\left(A'-3/2\right)\right\} \tag{19}$$

where x, y and z represent the coordinates of one end of the chain with respect to the other at quiescent condition, x', y' and z' are the relative coordination after stretching, k_{B} is the Boltzmann constant, $\beta = (3/2n)^{0.5}/l$ represents the reciprocal chain displacement value that is the most probable, l is the Kuhn length, n is the segment number per chain, ξ is the number of segments in the flow-induced crystalline phase, N_{c} is the total number of chains.

Considering the influence of orientation on the free energy of the initial melt, the parallel arrangement of the local stretched segments leads to the reduction in the number of possible conformations of the molecular chain, which is considered as the entropy effect. At the same time, there is an interaction between the parallel oriented segments, which manifests as an influence on enthalpy.[20] The entropy change of the melt caused by the oriented segments is defined as the orientation entropy, based on statistical mechanics and Maier-Saupe theory,[47] which can be expressed as

$$\Delta S_{\text{ori}} = -N_{\text{s}}k_{\text{B}}\left\langle \ln f(\phi)\right\rangle = -\frac{a_{\text{N}}}{V^2}\frac{N_{\text{s}}}{T}f^2 + N_{\text{s}}k_{\text{B}}\ln\left\{\int_0^1 \exp\left[-\frac{u(v,f)}{k_{\text{B}}T}\right]\mathrm{d}x\right\} \tag{20}$$

where N_{s} is the number of the ordered segments, $f(\phi)$ is the distribution function of the angle between segments and the stretching direction, a_{N} is a constant related to the mean field, V is the molar volume of the polymer, f is the Hermans' orientation parameter, $u(v,f)$ is the internal energy of a segment, and v is the segment vector. Considering that the change of volume of the polymer melt under deformation can be ignored, the enthalpy change of the melt induced by flow $\Delta H_{\text{f}}^{\text{l}}$ equals the internal energy change due to N_{s} oriented segments,[20,47] which can be expressed as

$$\Delta H_{\text{f}}^{\text{l}} = \Delta U_{\text{ori}} = \frac{1}{2}N_{\text{s}}\frac{a_{\text{N}}}{V^2}f^2 \tag{21}$$

Through Taylor expansion, ignoring higher-order terms, according to the Eqs. (20) and (21), the contribution of orientation to the free energy of the melt can be written as follows

$$\Delta G_{\text{ori}}^{\text{l}} = \Delta U_{\text{ori}} - T\Delta S_{\text{ori}} = af^2 + bf^3 + cf^4 \tag{22}$$

where a, b, and c are constants related to pressure and temperature.

The existence of crystals with different morphologies and structures under flow indicates that the existence of the enthalpy change of the crystal $\Delta H_{\text{f}}^{\text{c}}$ induced by flow, which can be obtained from the melting enthalpy of the different crystals.

DATA AVAILABILITY

The data that support the findings of this study are available from the corresponding author upon reasonable request.

ACKNOWLEDGMENTS

The work was financially supported by the National Natural Science Foundation of China (Nos. 51890872 and 51633009) and the National Key R&D Program of China (2018YFB0704200). The authors also appreciate the critical comments from Dr. Dong Liu (Mianyang), Dr. Nan Tian (Xian), Dr. Kunpeng Cui (Hokkaido) and Dr. Zhe Ma (Tianjin).

REFERENCES

1 Chandran, S.; Baschnagel, J.; Cangialosi, D.; Fukao, K.; Glynos, E.; Janssen, L. M. C.; Müller, M.; Muthukumar, M.; Steiner, U.; Xu, J.; Napolitano, S.; Reiter, G. Processing pathways decide polymer properties at the molecular level. *Macromolecules* **2019**, *52*, 7146−7156.

2 Cui, K.; Ma, Z.; Tian, N.; Su, F.; Liu, D.; Li, L. Multiscale and multistep ordering of flow-induced nucleation of polymers. *Chem. Rev.* **2018**, *118*, 1840−1886.

3 Lendlein, A.; Kelch, S. Shape-memory polymers. *Angew. Chem. Int. Ed.* **2002**, *41*, 2034−2057.

4 Wang, Z.; Ma, Z.; Li, L. Flow-induced crystallization of polymers: molecular and thermodynamic considerations. *Macromolecules* **2016**, *49*, 1505−1517.

5 Tang, X.; Chen, W.; Li, L. The tough journey of polymer crystallization: battling with chain flexibility and connectivity. *Macromolecules* **2019**, *52*, 3575−3591.

6 Graham, R. S. Understanding flow-induced crystallization in polymers: a perspective on the role of molecular simulations. *J. Rheol.* **2019**, *63*, 203−214.

7 Cui, K.; Liu, D.; Ji, Y.; Huang, N.; Ma, Z.; Wang, Z.; Lv, F.; Yang, H.; Li, L. Nonequilibrium nature of flow-induced nucleation in isotactic polypropylene. *Macromolecules* **2015**, *48*, 694−699.

8 Dukovski, I.; Muthukumar, M. Langevin dynamics simulations of early stage shish-kebab crystallization of polymers in extensional flow. *J. Chem. Phys.* **2003**, *118*, 6648−6655.

9 Liu, D.; Tian, N.; Cui, K.; Zhou, W.; Li, X.; Li, L. Correlation between flow-induced nucleation morphologies and strain in polyethylene: from uncorrelated oriented point-nuclei, scaffold-network, and microshish to shish. *Macromolecules* **2013**, *46*,

3435–3443.

10 Nicholson, D. A.; Rutledge, G. C. Molecular simulation of flow-enhanced nucleation in *n*-eicosane melts under steady shear and uniaxial extension. *J. Chem. Phys.* **2016**, *145*, 244903.

11 Yamamoto, T. Molecular dynamics simulation of stretch-induced crystallization in polyethylene: emergence of fiber structure and molecular network. *Macromolecules* **2019**, *52*, 1695–1706.

12 Tang, X.; Yang, J.; Tian, F.; Xu, T.; Xie, C.; Chen, W.; Li, L. Flow-induced density fluctuation assisted nucleation in polyethylene. *J. Chem. Phys.* **2018**, *149*, 224901.

13 Xie, C.; Tang, X.; Yang, J.; Xu, T.; Tian, F.; Li, L. Stretch-induced coil–helix transition in isotactic polypropylene: a molecular dynamics simulation. *Macromolecules* **2018**, *51*, 3994–4002.

14 Zhou, W.; Meng, L.; Lu, J.; Wang, Z.; Zhang, W.; Huang, N.; Chen, L.; Li, L. Inducing uniform single-crystal like orientation in natural rubber with constrained uniaxial stretch. *Soft Matter* **2015**, *11*, 5044–5052.

15 Nie, Y.; Zhao, Y.; Matsuba, G.; Hu, W. Shish-kebab crystallites initiated by shear fracture in bulk polymers. *Macromolecules* **2018**, *51*, 480–487.

16 Flory, P. J. Thermodynamics of crystallization in high polymers. I. Crystallization induced by stretching. *J. Chem. Phys.* **1947**, *15*, 397–408.

17 Doufas, A. K.; Dairanieh, I. S.; McHugh, A. J. A continuum model for flow-induced crystallization of polymer melts. *J. Rheol.* **1999**, *43*, 85–109.

18 Coppola, S.; Grizzuti, N.; Maffettone, P. L. Microrheological modeling of flow-induced crystallization. *Macromolecules* **2001**, *34*, 5030–5036.

19 Read, D. J.; McIlroy, C.; Das, C.; Harlen, O. G.; Graham, R. S. PolySTRAND model of flow-induced nucleation in polymers. *Phys. Rev. Lett.* **2020**, *124*, 147802.

20 Chen, X.; Meng, L.; Zhang, W.; Ye, K.; Xie, C.; Wang, D.; Chen, W.; Nan, M.; Wang, S.; Li, L. Frustrating strain-induced crystallization of natural rubber with biaxial stretch. *ACS Appl. Mater. Interfaces* **2019**, *11*, 47535–47544.

21 Nicholson, D. A.; Rutledge, G. C. An assessment of models for flow-enhanced nucleation in an *n*-alkane melt by molecular simulation. *J. Rheo.* **2019**, *63*, 465.

22 Zhang, W.; Larson, R. G. Effect of flow-induced nematic order on polyethylene crystal nucleation. *Macromolecules* **2020**, *53*, 7650–7657.

23 Wang, Z.; Ju, J.; Yang, J.; Ma, Z.; Liu, D.; Cui, K.; Yang, H.; Chang, J.; Huang, N.; Li, L. The non-equilibrium phase diagrams of flow-induced crystallization and melting of polyethylene. *Sci. Rep.* **2016**, *6*, 32968.

24 Liu, D.; Tian, N.; Huang, N.; Cui, K.; Wang, Z.; Hu, T.; Yang, H.; Li, X.; Li, L. Extension-induced nucleation under near-equilibrium conditions: the mechanism on the transition from point nucleus to shish. *Macromolecules* **2014**, *47*, 6813–6823.

25 Balzano, L.; Kukalyekar, N.; Rastogi, S.; Peters, G. W.; Chadwick, J. C. Crystallization and dissolution of flow-induced precursors. *Phys. Rev. Lett.* **2008**, *100*, 048302.

26 Cui, K.; Meng, L.; Tian, N.; Zhou, W.; Liu, Y.; Wang, Z.; He, J.; Li, L. Self-acceleration of nucleation and formation of shish in extension-induced crystallization with strain beyond fracture. *Macromolecules* **2012**, *45*, 5477–5486.

27 Barham, P. J.; Keller, A. High-strength polyethylene fibres from solution and gel spinning. *J. Mater. Sci.* **1985**, *20*, 2281–2302.

28 Cui, K.; Ma, Z.; Wang, Z.; Ji, Y.; Liu, D.; Huang, N.; Chen, L.; Zhang, W.; Li, L. Kinetic process of shish formation: from stretched network to stabilized nuclei. *Macromolecules* **2015**, *48*, 5276–5285.

29 Hu, W.; Frenkel, D.; Mathot, V. Simulation of shish-kebab crystallite induced by a single prealigned macromolecule. *Macromolecules* **2002**, *35*, 7172–7174.

30 Kanaya, T.; Matsuba, G.; Ogino, Y.; Nishida, K.; Shimizu, H. M.; Shinohara, T.; Oku, T.; Suzuki, J.; Otomo, T. Hierarchic structure of shish-kebab by neutron scattering in a wide *Q* range. *Macromolecules* **2007**, *40*, 3650–3654.

31 Ma, Z.; Balzano, L.; Peters, G. W. M. Dissolution and re-emergence of flow-induced shish in polyethylene with a broad molecular weight distribution. *Macromolecules* **2016**, *49*, 2724–2730.

32 Pennings, A. J.; Kiel, A. M. Fractionation of polymers by crystallization from solution, III. On the morphology of fibrillar polyethylene crystals grown in solution. *Kolloid-Zeitschrift und Zeitschrift für Polymere* **1965**, *205*, 160–162.

33 Pennings, A. J.; Lageveen, R.; de Vries, R. S. Hydrodynamically induced crystallization of polymers from solution. *Colloid Polym. Sci.* **1977**, *255*, 532–542.

34 Muthukumar, M. Nucleation in polymer crystallization. *Adv. Chem. Phys.* **2003**, *128*, 1–63.

35 Graham, R. S.; Olmsted, P. D. Coarse-grained simulations of flow-induced nucleation in semicrystalline polymers. *Phys. Rev. Lett.* **2009**, *103*, 115702.

36 Hassan, M. K.; Cakmak, M. Strain-induced crystallization during relaxation following biaxial stretching of PET films: a real-time mechano-optical study. *Macromolecules* **2015**, *48*, 4657–4668.

37 Wang, Z.; Su, F.; Ji, Y.; Yang, H.; Tian, N.; Chang, J.; Li, L. Transition from chain- to crystal-network in extension induced crystallization of isotactic polypropylene. *J. Chem. Phys.* **2017**, *146*, 014901.

38 Nie, Y.; Gao, H.; Yu, M.; Hu, Z.; Reiter, G.; Hu, W. Competition of crystal nucleation to fabricate the oriented semi-crystalline polymers. *Polymer* **2013**, *54*, 3402–3407.

39 Milner, S. T. Polymer crystal–melt interfaces and nucleation in polyethylene. *Soft Matter* **2011**, *7*, 2909–2917.

40 Balzano, L.; Rastogi, S.; Peters, G. W. M. Crystallization and precursors during fast short-term shear. *Macromolecules* **2009**, *42*, 2088–2092.

41 Keller, A.; Hikosaka, M.; Rastogi, S.; Toda, A.; Barham, P. J.; Goldbeck-Wood, G. An approach to the formation and growth of new phases with application to polymer crystallization: effect of finite size, metastability, and Ostwald's rule of stages. *J. Mater. Sci.* **1994**, *29*, 2579–2604.

42 Kwon, Y. K.; Boller, A.; Pyda, M.; Wunderlich, B. Melting and heat capacity of gel-spun, ultra-high molar mass polyethylene fibers. *Polymer* **2000**, *41*, 6237–6249.

43 Rastogi, S.; Kurelec, L.; Lemstra, P. J. Chain mobility in polymer systems: on the borderline between solid and melt. 2. Crystal size influence in phase transition and sintering of ultrahigh molecular weight polyethylene *via* the mobile hexagonal phase. *Macromolecules* **1998**, *31*, 5022–5031.

44 Krigbaum, W. R.; Roe, R. J. Diffraction study of crystallite orientation in a stretched polychloroprene vulcanizate. *J. Polym. Sci., Part A: Genr. Papers* **1964**, *2*, 4391–4414.

45 Yeh, G. S. Y.; Hong, K. Z. Strain-induced crystallization, Part III: Theory. *Polym. Eng. Sci.* **1979**, *19*, 395–400.

46 Yeh, G. S. Y.; Hong, K. Z.; Krueger, D. L. Strain-induced crystallization, Part IV: Induction time analysis. *Polym. Eng. Sci.* **1979**, *19*, 401–405.

47 Maier, W.; Saupe, A. Eine einfache molekular-statistische Theorie der nematischen kristallinflüssigen Phase. Teil II. *Zeitschrift Naturforschung Teil A* **1959**, *14*, 882.